RSC Advances

PAPER

View Article Online
View Journal | View Issue

Cite this: *RSC Adv.*, 2025, **15**, 49227

Pyrazine-driven dinuclear assembly of dysprosium(III) β-diketonate complex: a fluxidentate bridging approach toward functional near-white luminescent materials

Vandana Aggarwal,[a] Devender Singh,[*ab] Sonia Redhu,[a] Shri Bhagwan,[a] Sumit Kumar,[c] Rajender Singh Malik,[c] Parvin Kumar,[d] Jayant Sindhu[e] and Varun Kumar[f]

Three single component Dy(III) complexes featuring β-diketone ligand TTBD (4,4,4-trifluoro-1-(2-thienyl)-1,3-butanedione) were studied for their potential as white-light emitters. The complexes include a water-containing species (DyA) and two anhydrous species (DyM and DyD) incorporating the auxiliary bidentate ligand pyrazine (pyz). The coordination geometry and ligand environment, particularly the nuclearity and presence of sensitizing co-ligands, significantly influence the relative intensities of the characteristic Dy(III) yellow $^4F_{9/2} \rightarrow {}^6H_{13/2}$ and blue $^4F_{9/2} \rightarrow {}^6H_{15/2}$ and ligand-based phosphorescence emissions. The introduction of pyrazine enhances energy transfer efficiency, leading to improved Dy(III) emission output. Chromaticity coordinates measured at RT indicate that DyA (0.339, 0.336), DyM (0.404, 0.428) and DyD (0.323, 0.367) emit light close to the ideal white light coordinates (0.333, 0.333) as defined by the CIE system. Corresponding CCT values further classify DyA (5202 K) and DyD (5845 K) as cool white emitters, while DyM (3786 K) lies within the neutral-yellowish range. Emission branching ratio (β_R) analysis reveals that the $^4F_{9/2} \rightarrow {}^6H_{13/2}$ transition dominates (>90%), suggesting its suitability for laser amplification applications. In addition to their visible-light emission, the Dy(III) complexes exhibit good thermal stability and semiconducting characteristics, as confirmed by thermogravimetric (TG) and UV-Vis studies, respectively. Collectively, these findings support the potential application of these Dy(III) complexes as efficient, single component emitters for white light emitting devices (WLEDs).

Received 7th August 2025
Accepted 9th November 2025

DOI: 10.1039/d5ra05762k

rsc.li/rsc-advances

1 Introduction

Complexes of trivalent Ln(III) ions have been widely investigated due to their remarkable luminescent and magnetic properties, which support their broad range of applications including luminescent materials,[1] telecommunications,[2] photonics,[3] automotive catalysts,[4] glass manufacturing[5] and biomedical diagnostics[6] such as MRI, fluoroimmunoassays and nano-thermometry.[7] Development of new Ln(III) centered materials often influences their structural flexibility, which enables the fine tuning of their properties through controlled modifications of structure and electronic environment. This tunability can be achieved by varying ligand types, metal ion combinations, coordination numbers and the physical state (solid or solution). Typically, Ln(III) ions exhibit coordination numbers of 8 or 9,[8] which can be influenced by factors such as ligand bulkiness and the specific lanthanide ion employed. These structural changes not only impact geometry but also modulate luminescent properties. Ln(III) complexes are characterized by long emission lifetimes (in the ms range) and emission wavelengths that are relatively insensitive to environmental factors (*e.g.* ligand structure, co-ligands, solvents or physical state), providing them with distinct optical features.[9]

Compared to Eu-based single component white light emissive complexes, Dy-based complexes offer several notable advantages. Dy(III) ions exhibit characteristic emissions in both the blue (~480 nm, from the $^4F_{9/2} \rightarrow {}^6H_{15/2}$ transition) and yellow (~575 nm, from the $^4F_{9/2} \rightarrow {}^6H_{13/2}$ transition) regions, enabling efficient generation of white light from a single species without the need for multiple dopants or complex blending strategies.[10–13] This dual emission facilitates better color

[a]*Department of Chemistry, Maharshi Dayanand University, Rohtak-124001, Haryana, India. E-mail: devjakhar@gmail.com*

[b]*Department of Chemistry, Lovely Professional University, Phagwara, Jalandhar, Punjab, 14441, India*

[c]*Department of Chemistry, DCR University of Science & Technology, Murthal-131039, Haryana, India*

[d]*Department of Chemistry, Kurukshetra University, Kurukshetra-136119, Haryana, India*

[e]*Department of Chemistry, COBS&H, CCS Haryana Agricultural University, Hisar-125004, Haryana, India*

[f]*University Institute of Engineering and Technology (UIET), India*

balance and tunability of the emitted light color, which is often challenging to achieve in Eu(III) based systems that predominantly emit in the red region.[10,12] Furthermore, Dy(III) based complexes can exhibit shorter emission lifetimes and higher quantum yields under certain conditions, making them promising candidates for applications requiring rapid response times.[11,13] Additionally, Dy(III) salt is generally more abundant and less costly than Eu(III) salt, which is economically advantageous for large scale applications.[10] These characteristics have been discussed in recent comprehensive reviews and studies,[10–13] highlighting the potential of Dy(III) based complexes as efficient single component white light emitters.

A promising strategy in the design of new Ln(III)-based materials involves incorporating two or more metal centers, leading to di- or polynuclear structural design. Interionic interactions in such systems can give rise to enhanced photostability and emergent luminescent behavior.[14] Binuclear complexes, in particular, serve as useful platforms for modulating ion–ion, ion–ligand and ligand–ligand interactions, thereby offering access to novel properties.[15] Among the various ligands employed, polyazine type ligands are especially attractive owing to their chelating ability, thermal and chemical stability and adaptability in bridging coordination. Their ability to function as mono- or bi/polydentate ligands facilitates the synthesis of multinuclear lanthanide complexes. The preferred mode of polyazine coordination is influenced by the identity of the lanthanide ion, the co-ligands involved and the metal-to-ligand ratio used in synthesis. Despite their apparent structural simplicity, dinuclear lanthanide complexes display diverse architectures and coordination behaviors.[16]

In this context, 4,4,4-trifluoro-1-(2-thienyl)-1,3-butanedione (TTBD) was employed as a primary ligand for Dy(III) ion, which remains coordinatively unsaturated after initial complexation. Typically, remaining coordination sites are occupied by solvent molecules bearing O–H or N–H oscillators that quench luminescence *via* nonradiative relaxation. To diminish this, neutral ligand such as pyrazine is introduced to complete the coordination sphere and enhance photophysical performance. In this present article, the authors report the synthesis and characterization of mono- and dinuclear Dy(III) complexes using TTBD as the main ligand. The study includes elemental analysis, FT-IR, ^{1}H-NMR, UV-Vis and photoluminescence spectroscopy along with thermal analysis. Prepared complexes are: (i) (DyA) $[Dy(TTBD)_3(H_2O)_2]$, a binary mononuclear complex with eight coordinate geometry, (ii) (DyM) $[Dy(TTBD)_3(pyz)_2]$, another mononuclear species, where pyrazine acts as a monodentate neutral ligand and (iii) (DyD) $[Dy_2(TTBD)_6(pyz)]$, a dinuclear complex in which pyrazine bridges two Dy(III) centers, yielding a seven coordinate environment. A comprehensive comparison of their photophysical behaviors is presented, highlighting how coordination number and ligand environment influence luminescent properties.

2 Materials and techniques

The complexes DyA, DyM and DyD were synthesized using dysprosium(III) chloride hexahydrate ($DyCl_3 \cdot 6H_2O$), TTBD and pyz. All reagents were purchased from Aldrich with stated purity of 99.9%, 99% and ≥99%, respectively. Solvents utilized in the synthesis including hexane, ethanol and a 25% ammonia solution were of spectroscopic or analytical grade (SR/AR) and were used as received without further purification.

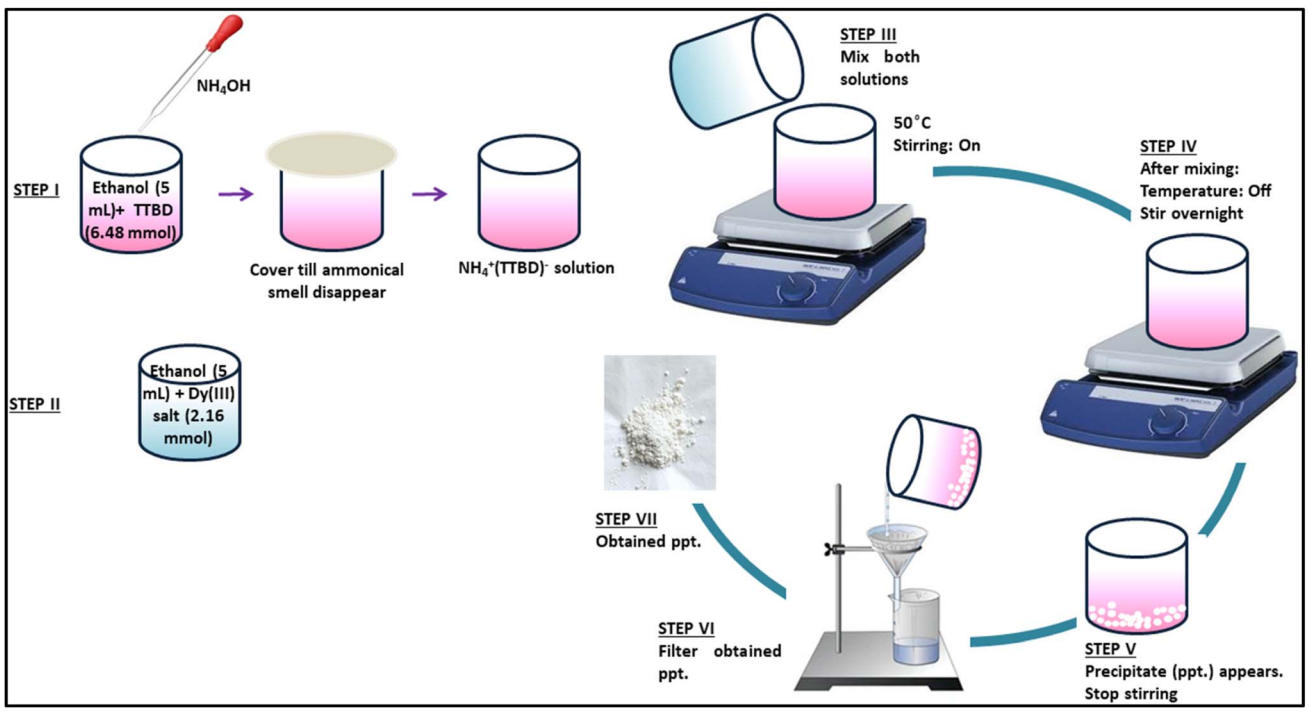

Fig. 1 Synthesis pathway for DyA.

Elemental analyses (CHN) of the synthesized complexes were performed using PerkinElmer 2400 Series II Elemental Analyzer. Powder XRD patterns were captured using Rikagu Ultima X-ray diffractometer irradiated with Cu/Kα rays (λ = 0.154 nm). Infrared (IR) spectra in the 400–4000 cm^{-1} region were taken on PerkinElmer 5700 FTIR spectrometer. ^{1}H NMR profiles were acquired on Bruker Avance Series II 400 MHz NMR spectrometer, using TMS as an internal reference and dichloromethane (DCM, 0.005 M) as the solvent. Electronic absorption profiles of TTBD and the synthesized complexes were obtained in DCM solution using Shimadzu UV-2450 spectrophotometer. Photoluminescence (PL) excitation and emission spectra were recorded in solution phase (DCM) on Horiba Jobin Yvon Fluorolog FL-3–11 spectrofluorometer. Luminescence lifetimes due to the most stable emissive states were measured using Hitachi F-7000 Fluorescence spectrophotometer at a 20 ms scan interval. Thermal stability was assessed through thermogravimetric analysis using a Hitachi STA-7300 system, at a heating rate of 10 °C min^{-1} under nitrogen atmosphere.

3 Synthesis

Present complexes DyA–DyD were synthesized by the procedure described in Fig. 1–3, respectively.[17–19]

4 Results and discussion

4.1 CHN analysis and PXRD

The synthesized mononuclear binary (DyA) and ternary (DyM) complexes with TTBD appeared as white to off-white solids, whereas the dinuclear complex incorporating pyrazine as a bridging ligand exhibited a yellowish-white color. Empirical formulae were proposed based on elemental (CHN) analysis and the experimentally determined values were found to be in excellent agreement with theoretical calculations, with minimal deviations, thereby approving the correctness of compositions. Table 1 summarizes the experimental (E) and theoretical (T) % of carbon, nitrogen and hydrogen, along with the corresponding molecular formulae and their abbreviated labels, which will be used consistently throughout the text. The dinuclear precursor complex was notably hygroscopic. It also demonstrated greater solubility compared to its mononuclear counterparts, in addition to exhibiting superior thermal stability.[20] The proposed structures derived from the elemental analysis data are illustrated in Fig. 4. Fig. S1 (in SI) depicts the diffractograms of DyA–DyD complexes. The diffraction patterns were recorded at Bragg's angle (2θ) within a range of 5–40° to get an idea about crystallinity of prepared complexes. X-ray diffraction patterns of DyA–DyD exhibited sharp peaks suggesting that these complexes are crystalline in nature and possess high degree of crystallinity. Their distinct XRD profiles indicate that they possess different degree of crystallinity. Similar results have been reported previously in literature which indicates that absence of well-resolved peaks is evident for low crystallinity of complexes.[21,22]

4.2 IR study

Infrared study was employed to ascertain functional groups in free ligands and to monitor spectral shifts indicative of metal coordination in the synthesized complexes. Key vibrational regions for both free and coordinated ligands are summarized

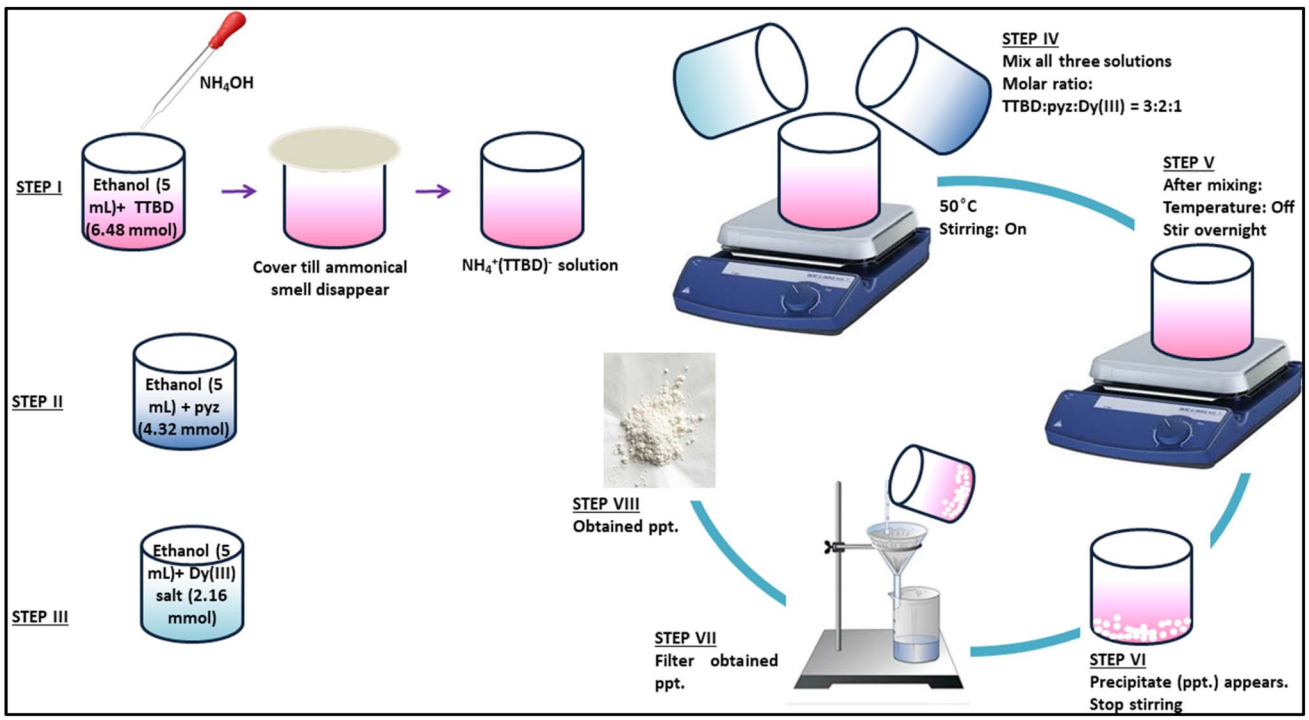

Fig. 2 Synthesis pathway for DyM.

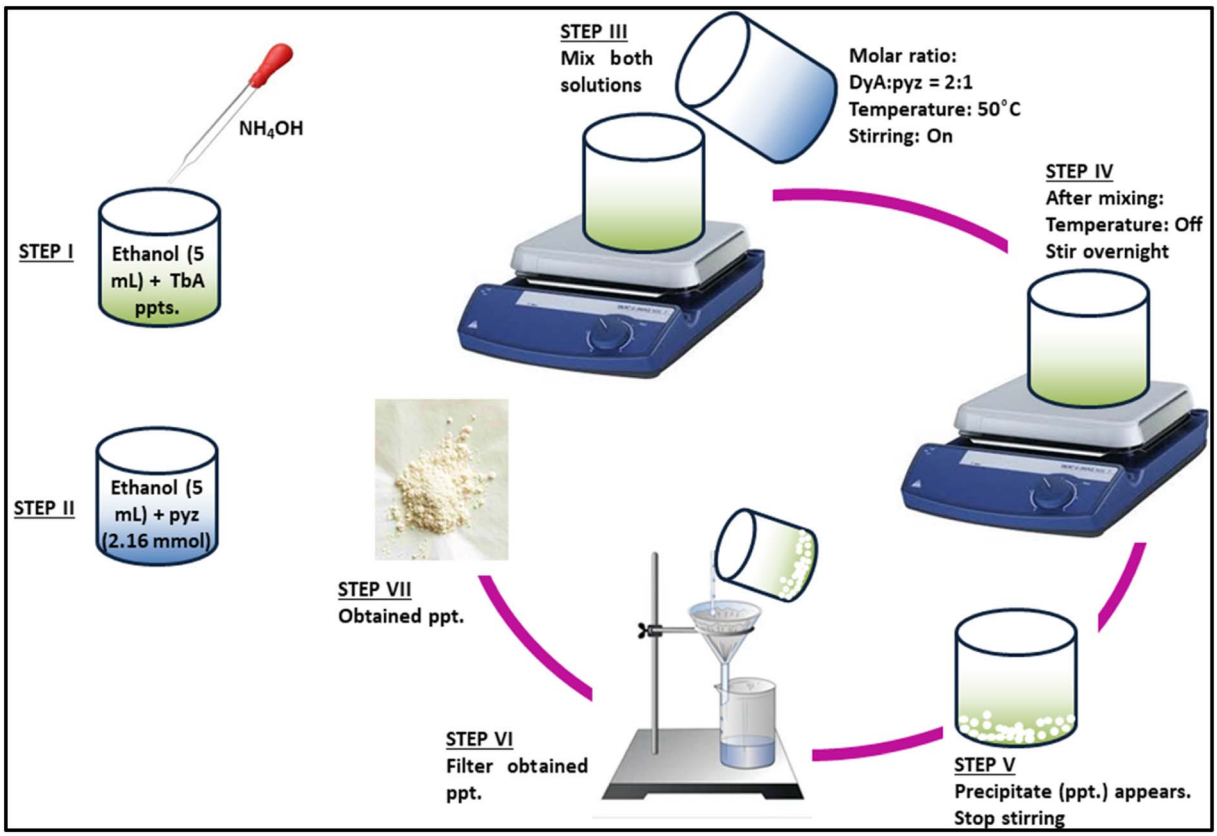

Fig. 3 Synthesis pathway for DyD.

in Table 2 and FTIR spectra of DyA–DyD have been displayed as Fig. S2–S4 (in SI), respectively. Upon complexation, red shifts were observed in several characteristic bands, confirming coordination between the ligands and Dy(III) ions. Notably, bands near 460 cm^{-1}, 580 cm^{-1} in pyz coordinated systems (DyM and DyD) were attributed to Dy–O (strong intensity) and Dy–N (weaker intensity) stretching modes, respectively.[23] A significant shift in C=O stretching vibration from 1655 cm^{-1} in free TTBD to ~1590 cm^{-1} in complexes further supports metal coordination.[24] The IR spectra of DyM and DyD also displayed characteristic vibrations (in cm^{-1}) for CH (~2900), C=N (~1540) and C–N (~1358), along with aromatic C–H deformation modes in the 767–771 cm^{-1} region.[25,26]

In the binary complex (DyA), a band in 1645–1623 cm^{-1} range was consigned to the $\delta_{(OH)}$ bending of coordinated water.[27] It also featured a broad O–H stretching band around 3200 cm^{-1}, indicative of coordinated water. For DyD, the carbonyl stretching frequency (in cm^{-1}) translocate from 1604 (in DyA) to 1604 (in DyM) and 1597 (in DyD), indicating coordination of the bridging pyrazine ligand. Likewise, C=N stretching band of free pyz at 1605 cm^{-1} shifted to ~1540 cm^{-1} upon complexation in DyM and DyD, confirming the involvement of nitrogen atoms in coordination with Dy(III). Strong $\nu_{(C=N)}$ bands appeared in the 1553 cm^{-1} region for DyM, with the dinuclear species showing a slight shift to lower wavenumbers (1531 cm^{-1}), consistent with altered electronic environments upon dinuclear coordination. Further evidence of metal–ligand interaction is provided by the shift of the symmetric CF_3 stretching band ($\nu_s(CF_3)$) to 1140 cm^{-1} in the complexes.

4.3 ^{1}H-NMR study

NMR spectroscopy provided strong evidence for the successful formation of dinuclear complex. In the spectrum of free pyz, a single resonance appears at 8.5 ppm.[28] The TTBD ligand exhibits characteristic signals for its thiophene ring at 7.84, 7.60 and 7.20 ppm, along with a sharp singlet due to the methine proton (6.45 ppm) and an enolic proton signal at 14.9 ppm.[29] The observed peak intensities follow the expected 1 : 1 : 1 : 1 : 1 ratio. All relevant proton magnetic resonance (PMR) signals are summarized in Table 3. In DyM, coordination of pyz results in

Table 1 % CHN content (E and T) in DyA–DyD

Complex	Color	C_E (T)	H_E (T)	N_E (T)	Formula
DyA	White	33.47 (33.44)	1.93 (1.87)	—	$C_{24}H_{16}DyF_9O_8S_3$
DyM	Off-white	39.02 (38.97)	1.97 (2.04)	5.63 (5.68)	$C_{32}H_{20}DyF_9N_4O_6S_3$
DyD	Pale yellow	36.13 (36.06)	1.52 (1.63)	1.59 (1.62)	$C_{52}H_{28}Dy_2F_{18}N_2O_{12}S_6$

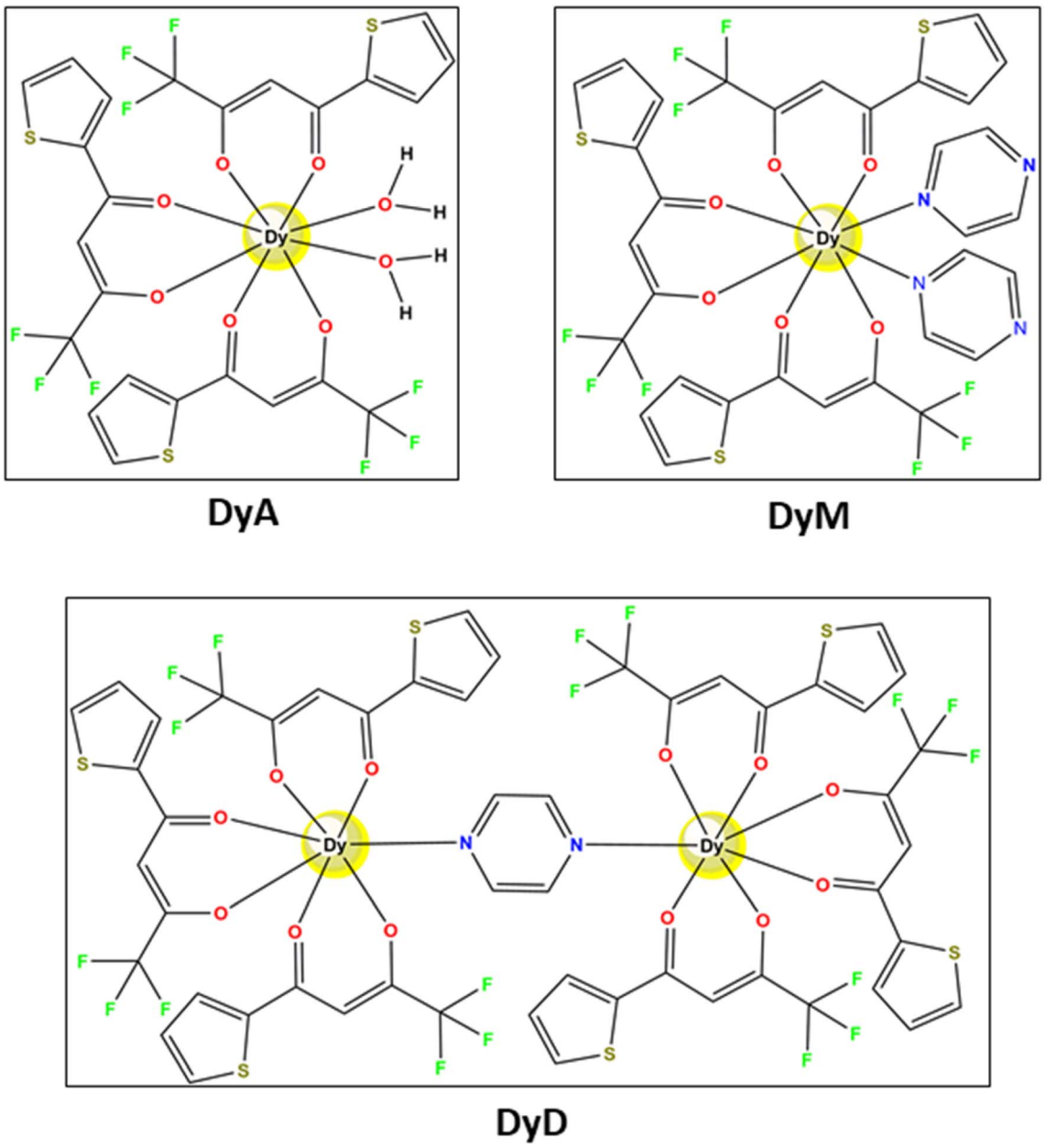

Fig. 4 Structure of prepared complexes.

Table 2 IR data of free ligands and prepared complexes (in cm^{-1})

Complex	TTBD	pyz	DyA	DyM	DyD
$\nu_{(Dy-O)}$	—	—	461	461	461
$\nu_{(Dy-N)}$	—	—	—	579	579
$\nu_{(C-F)}$	—	—	1140, 1192	1140, 1184	1140, 1192
$\nu_{(C-N)}$	—	—	—	1361	1338
$\nu_{(C=C)}$	—	1457	1459	1449, 1508	1457, 1494
$\nu_{(C=N)}$	—	—	—	1553	1531
$\nu_{(C=O)}$	1655	—	1604	1604	1597
$\nu_{(=CH)}$	—	—	2909	2902	2907

notable upfield shifts. These shifts, relative to the free ligand, confirm coordination of pyz to Dy(III) ion. The intensity ratio of 3 : 8 among the methine protons of TTBD and pyrazine protons supports a structure in which Dy(III) is coordinated to three TTBD units and two pyz molecules, consistent with an eight-coordinate geometry. Additionally, the observation of two equally intense signals from pyrazine supports its monodentate binding mode in this complex.

For complex DyD, the PMR spectrum is consistent with a pyrazine-bridged dinuclear structure. The paramagnetic nature of the complex $[(TTBD)_3Dy(\mu\text{-pyz})Dy(TTBD)_3]$ results in three distinct signals: two attributed to TTBD and one to pyrazine, in an intensity ratio of 18 (thienyl) : 6 (methine) : 4 (pyz). The signal at 177.58 ppm (δ), integrating for six protons, due to the methine groups of the TTBD ligands. In the aromatic region, a singlet at −54.48 ppm (δ) integrates for four protons and is assigned to pyrazine. This signal is shifted highly upfield

Table 3 PMR signals of prepared complexes in ppm

Complex	Peaks due to TTBD	Peaks due to pyz
Uncoordinated	14.9 (1H), 7.84 (1H), 7.60 (1H), 7.20 (1H), 6.45 (1H)	8.50 (4H)
DyA	157.63 (s), 7.22–7.86 (m)	—
DyM	162.16 (s), 7.24–7.90 (m)	−62.37 (s), −8.07 (s)
DyD	177.58 (s), 7.30–7.99 (m)	−54.48 (s)

relative to free pyrazine (8.50 ppm), indicating shielding due to coordination. The presence of a single resonance for pyrazine, rather than the two signals typical of monodentate coordination, confirms symmetrical bridging of the ligand between the two Dy(III) centers. Importantly, the chemical shifts of pyrazine and TTBD protons in these complexes move in opposite directions: pyrazine protons experience upfield shifts, while thiophene and methine protons of TTBD shift downfield. This contrasting behavior suggests dipolar interactions between the protons and the paramagnetic Dy(III) center.[30] The magnitude of the shift correlates with the proximity of the proton to the metal ion, decreasing with increasing distance, further supporting a dipolar origin of the observed shifts.

4.4 UV-vis spectroscopic Study

The UV-Vis spectrum of the free TTBD exhibits strong π–π* transitions, indicating its efficient UV light absorbing nature. TTBD shows two broad, intense absorption bands at 268 nm and 299 nm.[31] Pyrazine displays a singlet to singlet transition with a maximum at 275 nm in DCM (10^{-3} M).[32] These spectral features reflect the significant conjugation and electronic activity of ligands. Upon complexation with Dy(III), notable spectral shifts are observed (Fig. 5). The electronic absorption spectra of the resulting complexes show prominent bands centered at 273, 337 nm for DyA, 270, 341 nm for DyM and 275, 347 nm for DyD. These absorption features arise from the combined electronic transitions of TTBD and pyrazine and are red-shifted relative to the free ligands. This bathochromic shift indicates coordination of the ligands to the metal ion, which stabilizes the π* orbitals of TTBD and pyz, thus lowering the energy of the transitions. Table 4 summarizes the absorption maxima due to π → π* and n → π* transitions for TTBD, pyrazine and the synthesized complexes. No absorptions were observed in the visible region, suggesting an absence of metal to ligand charge transfer (MLCT) transitions. Interestingly, the UV-Vis spectrum of the Dy(TTBD)$_3$ complex closely resembles that of the bridged dinuclear Dy(III) complex, indicating that coordination of pyrazine as a bridging ligand between two Dy(TTBD)$_3$ units results in stabilization of the pyrazine π* orbitals and shifts their energy to lower values. This behavior is consistent with previous observations for other bridging ligands, such as dipyridyl–tetrazine, upon coordination with lanthanide ions.[33] Overall, the red-shifted absorption bands in the complexes as compared to free sensitizers are accredited to the expansion of π-conjugated system due to metal coordination.[34]

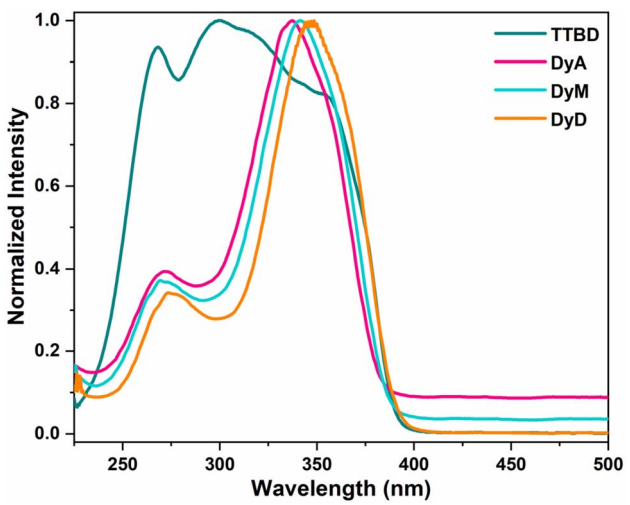

Fig. 5 Normalized electronic absorption graphs of TTBD and prepared complexes.

4.4.1 Band-gap determination. The band gap energy of a semiconductor represents the minimum energy required to promote an electron from the valence band to the conduction band. Accurate determination of this parameter is essential for understanding and predicting the photophysical behavior of semiconducting materials. In 1966, Tauc introduced a widely used method for estimating band gap energies, based on the relationship between the absorption coefficient (α) and photon energy.[35] According to the Tauc model on electronic absorption data obtained from UV spectroscopic study, the absorption coefficient follows theeqn(1):[36]

$$\alpha h\nu^{1/n} = A(h\nu - E_g) \quad (1)$$

where, h is Planck constant, ν is the photon frequency, E_g is the band gap energy, A is a material dependent constant and n is a factor determined by the nature of the electronic transition (1/2 for direct allowed transitions and 2 for indirect allowed transitions). Semiconductors typically exhibit a linear region in the Tauc plot, where absorption (from UV-analysis) increases sharply with photon energy. Extrapolating this linear portion to the energy axis yields an estimate of the band gap energy. In this study, the estimated band gap values are approximately 3.3 eV (Fig. 6), suggesting that the synthesized complexes possess semiconducting properties and may hold promise for opto-electronic or photonic applications.[37,38]

Table 4 Some optical parameters of prepared complexes

Complex	λ_{abs}	E_g	λ_{ex}	λ_{em}	Φ	Lifetime (μs)
DyA	273, 337	3.313	280, 380	574	0.03	0.040
DyM	270, 341	3.289	281, 377	575	0.17	0.184
DyD	275, 347	3.246	281, 378	573	0.12	0.146

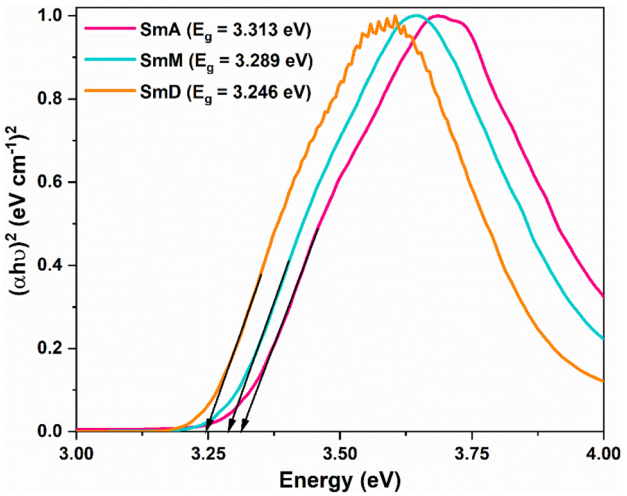

Fig. 6 Band-gap profiles of prepared complexes.

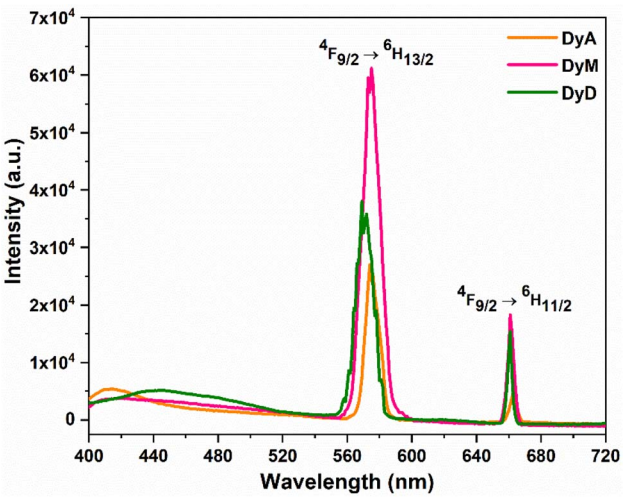

Fig. 8 Emission spectra of prepared complexes in DCM.

4.5 Photoluminescence spectroscopy

4.5.1 PL excitation and emission. Excitation profiles of DyA–DyD are presented in Fig. 7. When monitored at the characteristic emission wavelength of 574 nm ($^4F_{9/2} \rightarrow {}^6H_{13/2}$ transition), two broad and intense excitation bands are observed in the 260–400 nm range. Existence of this strong ligand centered band indicates effective energy transfer from sensitizer to Dy(III) center, particularly in DyD complex.[39,40] The excitation spectrum of the prepared complexes display two prominent bands centered around 275 nm and 375 nm, while the absorption spectrum similarly shows bands near 275 nm and 350 nm. These dual humps are consistent across repeated measurements, indicating their reproducibility and significance. Excitation spectrum of TTBD is displayed in Fig. S5 (in SI). The band near 275 nm is assigned to $\pi \rightarrow \pi^*$ transitions of the aromatic or conjugated ligand system, while the lower energy band around 350–375 nm is likely due to $n \rightarrow \pi^*$ transitions. The close match between excitation and absorption spectra further supports this assignment, suggesting efficient energy transfer from the ligand excited states to the Dy(III) center. Such dual band features are commonly reported in similar lanthanide complexes[41] and they reflect the complex photophysical behavior of the organic ligands in coordination with the metal center.

The emission spectra of the solvated Dy(III) complexes, recorded under their respective excitation wavelengths, are shown in Fig. 8. All three complexes (DyA–DyD) exhibit characteristic dysprosium emission peaks at 481, 575 and 662 nm, due to $^4F_{9/2} \rightarrow {}^6H_{J/2}$ where, J = 15, 13 and 11, respectively. Among these, the 575 nm transition considered hypersensitive due to its strong dependence on the local coordination environment appears as the most intense and primarily governs the overall emission color.[42] A broad ligand based phosphorescence band centered around 410–440 nm is also observed at room temperature, attributed to the TTBD ligand (Fig. S5, in SI).[43] Notably, all of the complexes exhibited a ligand based band, confirming that the UV radiation absorbed by TTBD was emitted directly by the ligand itself but was not effectively transferred to the metal ion. The lowest emission intensity of peaks and most intense emission band is noted for DyA, likely due to luminescence quenching caused by O–H vibrational modes of coordinated water and the relatively low lying triplet state of TTBD.[44,45] In contrast, water free complexes (DyM and DyD) display lower intensity of the broad ligand based band and enhanced metal centered emission, highlighting the beneficial role of pyrazine coordination.

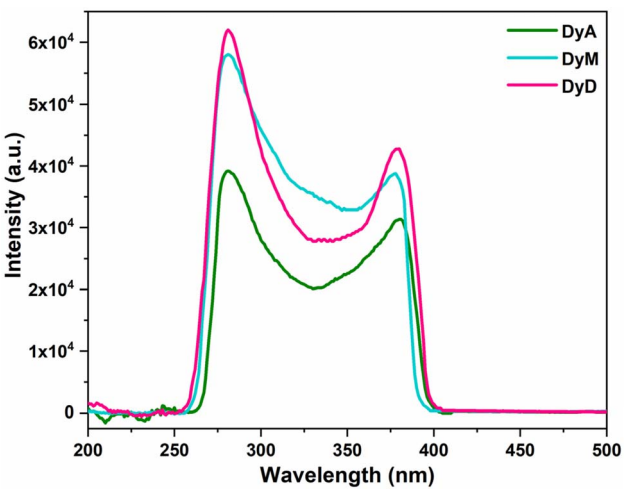

Fig. 7 Excitation spectra of prepared complexes in DCM.

Table 5 Branching ratio (%) of prepared complexes[a]

	Branching ratio ($^4F_{9/2} \rightarrow {}^6H_{J/2}$)		
Complex	J = 15	J = 13	J = 11
DyA	—	91.66	8.33
DyM	—	90.14	9.85
DyD	—	90.26	9.73

[a] merged with ligand based band.

Table 6 T_1 energy with its difference with emitting level of central ion

Complex	Energy (cm^{-1})
E_{pyz}	26 820
E_{TTBD}	20 600
$E_{Dy(III)}$	20 833
$\Delta E_{TTBD\text{-}Dy(III)}$	−233
$\Delta E_{Pyz\text{-}Dy(III)}$	5987

Moreover, the introduction of pyrazine into the coordination environment provides three key advantages: (i) elimination of water molecules from the inner coordination sphere, thus reducing nonradiative quenching; (ii) enhanced energy transfer efficiency from both TTBD and pyrazine ligands to the Dy(III) ion, increasing metal centered luminescence relative to ligand emission and (iii) extension of π-conjugation *via* the pyrazine ligand, promoting more effective light absorption and energy transfer across the molecule. These effects contribute to a more efficient sensitization of Dy(III) in water free complexes. Although excitation spectra suggest that DyD undergoes the most effective energy absorption *via* ligand excitation, the highest emission intensity is observed for DyM. This enhanced luminescence is credited to the existence of two pyrazine units in DyM, in comparison to single bridging pyrazine in DyD. The increased efficiency likely arises from an optimal energy gap among the triplet state (T_1) of donor ligands and emitting state of Dy(III), which enables more effective energy transfer. Overall, considerable emission intensities observed in all three complexes confirm that TTBD effectively sensitizes the characteristic luminescence of Dy(III), despite its triplet state lying below the emissive excited state of metal.[46–48]

Branching ratio (β_R) is the key parameter in laser design, as it reflects the possibility of achieving stimulated emission from a particular radiative peak.[49] A higher β_R value indicates a greater potential for efficient stimulated emission and consequently, a more favorable stimulated emission cross section (SEC). β_R data for synthesized Dy(III) complexes are presented in Table 5. Among the observed transitions, the ratio follows $^4F_{9/2} \rightarrow {}^6H_{13/2} > {}^4F_{9/2} \rightarrow {}^6H_{11/2}$ trend. The dominant $^4F_{9/2} \rightarrow {}^6H_{13/2}$ transition exhibits a significantly higher branching ratio, accounting for approximately 90% of the total emission. This indicates that this transition is the most promising candidate for radiative amplification and is highly favorable for potential laser applications.[50]

4.5.2 Quantum yield. Photoluminescence quantum yield (PLQY), the ratio of photons emitted to photons absorbed, of prepared complexes were determined in DCM.[51] It helped in analyzing the effect of coordination environment on the photoluminescence intensity of metal center. It was evaluated using eqn (2) against quinine bisulphate (reference) in dil. H_2SO_4 having QY (Φ) equal to 0.546.[52,53]

$$\phi_s = \frac{\phi_r A_r I_r n_s^2}{A_s I_r n_r^2} \quad (2)$$

where the subscripts, s and r are for unknown sample and reference, respectively. I is integrated intensity of emission, A is the absorbance at excitation wavelength and n is refractive index. The notably high quantum yield value for DyM indicates a substantial sensitizing effect of pyz over TTBD for Dy(III) ion in prepared complexes. The quantum yield data is summarized in Table 4. The relative quantum yields are reported relative to a reference solution with a 10% error margin. The emission quantum yields for the complexes were found to be comparable to those reported previously for similar complexes.[54,55]

4.5.3 Emission mechanism. In the sensitization mechanism, efficient energy transfer from T_1 state of ligand to Ln ion emitting level involves four key steps: (i) excitation of organic chromophore from its ground state (S_0) to an excited singlet

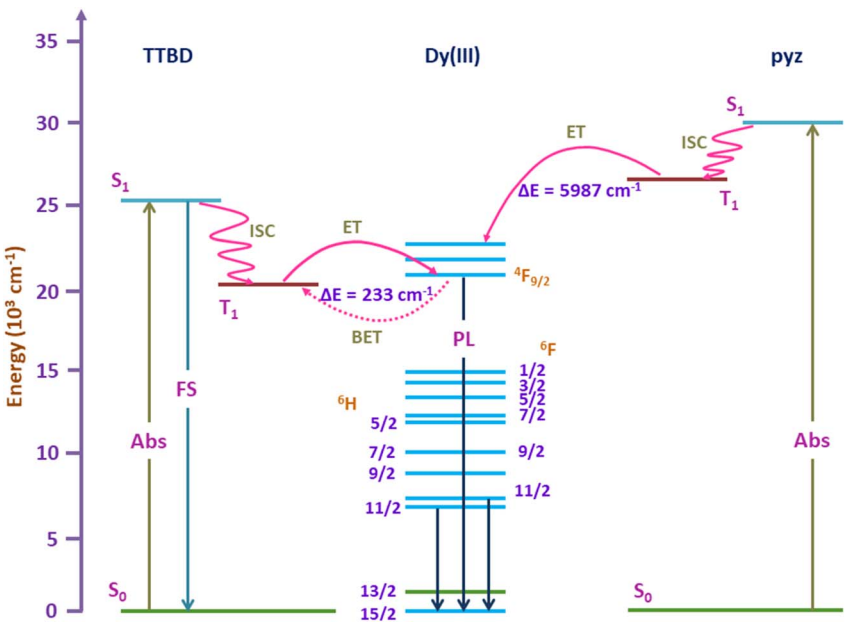

Fig. 9 Graphic presentation of probable energy-transfer occurring in DyA–DyD.

state (S_1) *via* UV-Visible radiation (ii) intersystem crossing (ISC) from S_1 of ligand to its T_1 (iii) nonradiative energy transfer from T_1 state of ligand to resonant excited states of Ln(III) ion and (iv) radiative emission from the Ln ion. Among these, the third step critically governs the luminescence efficiency of the lanthanide complex.[56] Beyond these steps, the existence of oscillators like –OH and –NH groups in coordination surrounding can severely quench luminescence by facilitating nonradiative decay and shortening the excited state lifetime of Ln(III) ions. Hence, for photophysical applications, Ln(III) complexes should ideally be free of coordinated water or other molecules containing such vibrational quenchers.

Emission study of DyA–DyD (Fig. 8) reveal a pronounced antenna effect in DyM and DyD, yielding yellow and near white emission, respectively. To fully understand the energy transfer dynamics, it is necessary to determine singlet and triplet energy levels of chromophore. The first excited triplet ($^3\pi\pi^*$) states of TTBD and pyz are located at 20 600 cm^{-1} and 26 820 cm^{-1}, respectively (Table 6).[57,58] The singlet-triplet energy gap of TTBD ~4564 cm^{-1} is in agreement with Reinhoudt empirical rule that requires a gap ~5000 cm^{-1} for efficient Intersystem Crossing.[59] Furthermore, T_1 energy of pyz (26 820 cm^{-1}) lies well above the Dy(III) emitting level ($^4F_{9/2}$ at 20 833 cm^{-1})[60] by about 5987 cm^{-1}, enabling efficient energy transfer in DyM and DyD. Conversely, the triplet level of TTBD (20 600 cm^{-1}) is slightly below (by 233 cm^{-1}) the Dy(III) emitting state, which accounts for the broad ligand centered emission observed in the complexes spectra. In water-free complexes, higher T_1 state of pyz makes it a more effective antenna for Dy(III) sensitization compared to TTBD. These findings explain the relatively stronger ligand based emission, especially in water containing complexes where coordinated water leads to less efficient ligand to metal energy transfer (Fig. 9). The overall energy transfer process is further supported by excitation spectra when Dy(III) ions are directly excited at their characteristic f–f sublevels, only ligand-related absorption bands (~280, 380 nm, $^1\pi\pi^*$ transition) are detected (Fig. 7). A schematic of the complete energy transfer pathway is illustrated in Fig. 9.

4.5.4 Decay time. Time resolved photoluminescence measurements (Fig. 10 and Table 4), carried out by monitoring the emission intensity at 574 nm, reveal that the decay profile of the Dy(III) $^4F_{9/2}$ excited state follows a monoexponential trend.

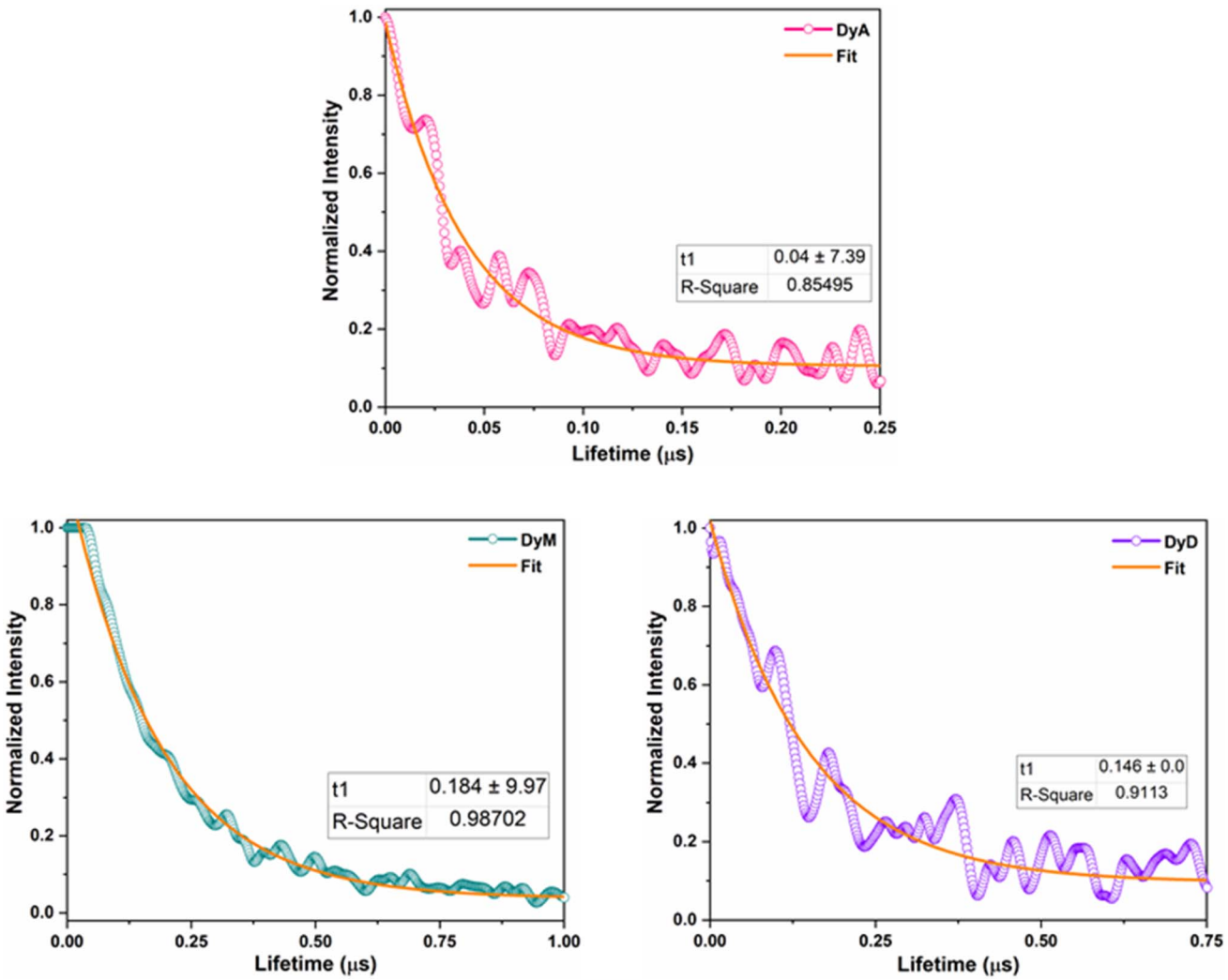

Fig. 10 Deactivation time-profiles of DyA–DyD.

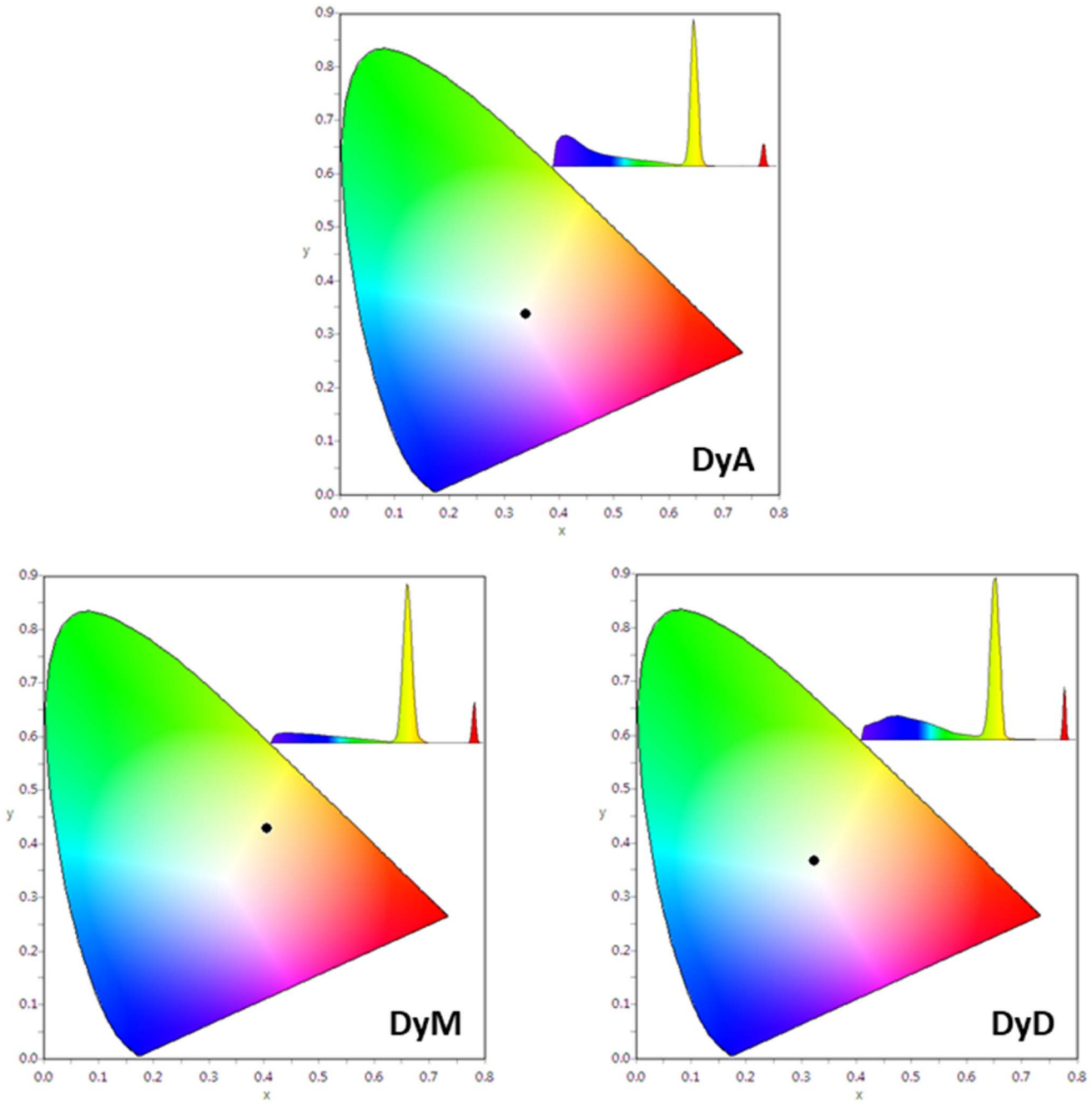

Fig. 11 CIE 1931 (*x*, *y*) plot of DyA–DyD with color contribution of each peak.

The single exponential nature of the decay indicates that there is a single, well-defined type of Dy(III) emissive center within the synthesized complexes, without contributions from multiple sites or environments. The observed reduction in the excited state lifetimes of DyA is consistent with the presence of coordinated water molecules, which are well known quenchers of lanthanide luminescence through vibrational energy transfer mechanisms.[61] This quenching effect manifests as a shortening of the $^4F_{9/2}$ level lifetime, as shown in the corresponding decay profiles (Fig. 10). When water moieties in coordination sphere are substituted by pyz ligand, the coordination environment of Dy(III) is altered significantly, resulting in notable changes in the emission intensity and lifetime parameters. Specifically, the substitution of water by pyz ligands reduces the nonradiative relaxation pathways, thereby enhancing the radiative decay probability and leading to increased luminescence lifetimes in the water-free complexes. This observation aligns well with the predicted quenching effect of O–H vibrational oscillators associated with coordinated water, which effectively deactivates excited states through multiphonon relaxation.

The discrepancy in lifetime values observed between the DyM and DyD complexes, despite the latter containing two Dy(III) centers, can be rationalized by subtle differences in the ligand coordination environment. DyD incorporates a higher

Table 7 (x, y) and (u', v') values of prepared complexes

Complex	DyA	DyM	DyD
x, y	0.339, 0.336	0.404, 0.428	0.323, 0.367
u', v'	0.213, 0.476	0.220, 0.526	0.191, 0.488
CCT (K)	5202	3786	5845

number of pyz ligands, which contribute to the more effective sensitization of Dy(III) ion *via* improved energy transfer processes. This highlights the essential role that ligand structure and coordination geometry play in modulating the photophysical properties and emission lifetimes of lanthanide complexes. Furthermore, present study demonstrates that homodinuclear Dy(III) complexes bridged by pyz exhibit longer excited state lifetimes than their mononuclear aquated analogues. This enhancement is attributed to two main factors (i) the effective bridging of two Dy(III) centers by the polyazine ligand, facilitating energy transfer and possibly exciton migration between metal centers and (ii) the elimination of O–H vibrational quenching channels due to absence of coordinated water moieties. Overall, these findings emphasize that the design of the coordination-sphere particularly the replacement of quenching water molecules with rigid, conjugated ligands such as pyz plays a critical role in enhancing the luminescence efficiency and excited state dynamics of Dy(III) based complexes, providing valuable insights for the development of high performance lanthanide based photonic materials.

4.5.5 Color modulation. Fig. 11 displays CIE chromaticity diagram of DyA–DyD, derived from their PL spectra recorded in solution state, while the corresponding chromaticity coordinates (x_e, y_e) are summarized in Table 7. CIE triangle clearly demonstrates that Dy(III) complexes exhibit distinct emission colors depending on their nuclearity. Based on the CIE coordinates presented in Table 7, the DyA and DyD complexes emit light that closely approximates pure white light, with chromaticity values near ideal white point of ($x = 0.333$ and $y = 0.333$). Conversely, the emission from the DyM complex shifts toward a neutral yellow region on the diagram. As illustrated in the CIE plot, tuning of the emission color was successfully achieved by altering the coordination environment through incorporation of the fluxidentate auxiliary pyz ligand. This modification enabled a controlled shift in the emission color from yellow in the mononuclear DyM complex to white light emission in the binuclear DyD complex. This color tunability correlates with an intensified residual blue emission originating from TTBD upon formation of dinuclear species. In the solution phase, white-light emission (WLE) from Dy(III) complex arises predominantly due to a balanced contribution of yellow and blue

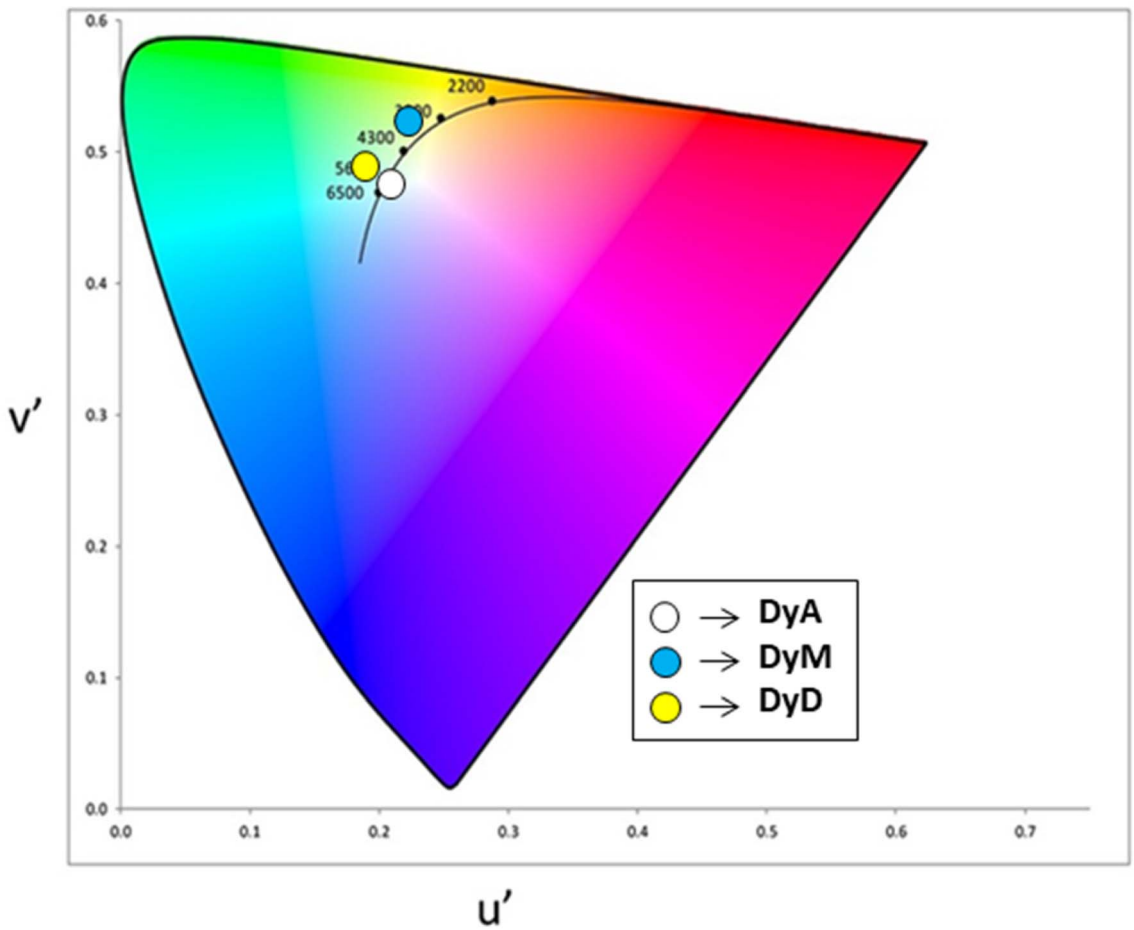

Fig. 12 CIE 1976 (u', v') plot of DyA–DyD.

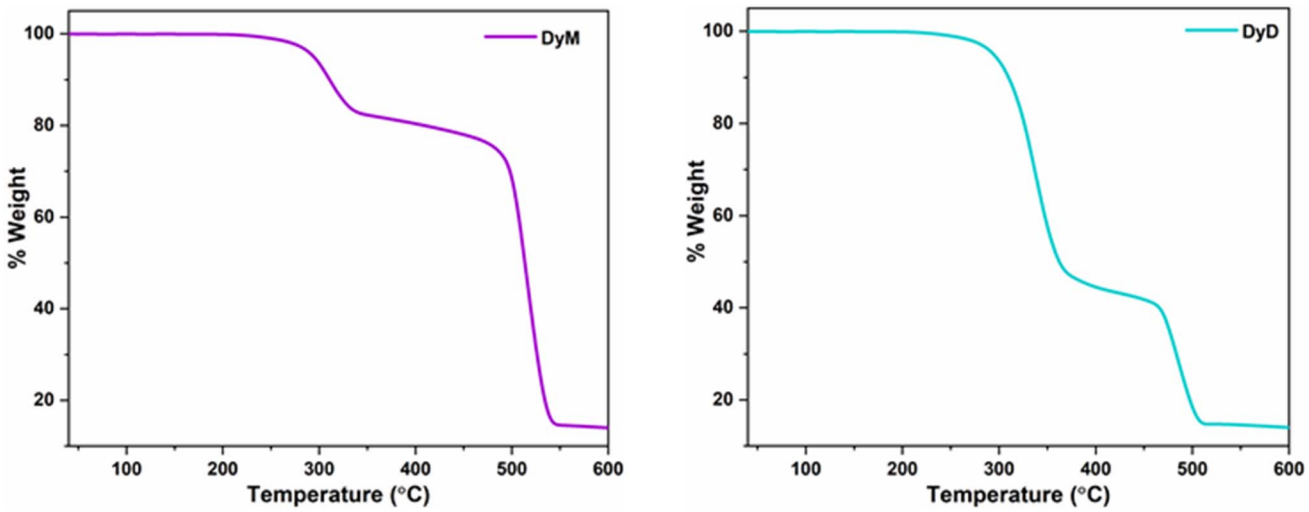

Fig. 13 TG profiles of DyM and DyD.

emission peaks. Shift in emitting color from white to yellow is possibly related to differing energy transfer dynamics in these complexes. Under conditions of efficient energy absorption, the antenna effect facilitates effective sensitization of the lanthanide ion by minimizing nonradiative losses, thereby enhancing lanthanide centered emission. Conversely, when absorbed energy is lost nonradiatively mainly through vibrational interactions with CH and OH oscillators present in the solvent, ligand fluorescence becomes more prominent and competes with Ln(III) based emission, producing a resultant blue emission. Therefore, by precisely modulating the relative intensities of Ln emission and ligand fluorescence, it is possible to finely tune the emission color of these lanthanide complexes, highlighting the significant part of the coordination environment and solvent interactions in controlling their photophysical performance. u' and v' data was determined by replacing the corresponding x, y data into eqn (3).[62] Obtained points have been plotted in CIE 1976 color chart (Fig. 12).

$$u' = \frac{4x}{-2x + 12y + 3}, v' = \frac{9y}{-2x + 12y + 3} \quad (3)$$

Analysis of quality of emitted light produced from prepared complexes was made using McCamy relation of correlated color temperature (CCT) by eqn (4).[63]

$$\mathrm{CCT} = -437n^3 + 3601n^2 - 6861n + 5514.31 \quad (4)$$

In eqn (4), n is reciprocal slope and is given by $\frac{(x - x_e)}{(y - y_e)}$. CCT values for prepared complexes are concised in Table 7. The measured CCT values for the DyA and DyD complexes (above 5000 K) in solution indicate emission within the cool white light region, closely resembling natural daylight.[63] This makes them ideal for lighting solutions in environments such as office waiting rooms, dressing areas and vanity tables where natural light like illumination is preferred. Based on this criterion, complexes DyA and DyD demonstrate strong potential as cold white light sources for practical lighting applications.[64]

4.6 TG/thermal analysis

The thermal stability of complexes DyA–DyD was investigated using thermogravimetric analysis (TGA).[65–67] Thermograms of water-free complexes (DyM, DyD) are displayed in Fig. 13. The TGA data reveal a two-step, slow weight loss pathway. For DyM, TGA curve shows an initial mass loss of 17.04% (calculated 16.25%) starting from 229 to 343 °C, which corresponds to the loss of two coordinated pyz molecules. Subsequently, second step starts at 459–551 °C, attributed to the dissociation of the TTBD ligands (calculated 83.82%). Finally, metal oxide (Dy_2O_3) is obtained as residue. A similar thermal profile was observed for DyD. It begins to decompose between 247 and 359 °C. A rapid and substantial weight loss of 48.16% occurs, attributed to the breakdown of pyrazine ligands (calculated 47.68%) is observed. Upon further heating above 448 °C, a mass loss of 79.84% (calculated 81.58%) due to the release of diketone moieties is noted between 448 and 512 °C.

5 Conclusions

A set of Dy(III) β-diketonate complexes comprising one water-containing species (DyA) and two water-free species (DyM and DyD) were synthesized using TTBD ligand in combination with pyrazine (pyz) as an auxiliary co-ligand. In the water-free complexes, pyrazine plays a dual role: acting as a monodentate ligand in DyM to form an eight coordinated mononuclear complex and serving as a bridging spacer in DyD, leading to the formation of a dinuclear species. Structural confirmation was achieved through elemental analysis, IR and ^{1}H NMR spectroscopy. All complexes demonstrate semiconducting behavior, as indicated by band gap estimations derived from UV-Vis absorption spectra. Luminescence studies reveal prominent emissions in the visible range, attributed to the characteristic $^4F_{9/2}$ transitions of Dy(III) ion. The close energy

match among T_1 states of TTBD and pyz with Dy(III) emissive level facilitates partial ligand-to-metal energy transfer, enabling simultaneous blue (ligand based) and yellow (Dy(III) based) emissions. This synergistic emission yields white light output from single component systems. Chromaticity coordinates of DyA (0.339, 0.336) and DyD (0.323, 0.367) fall near the ideal white light point (0.333, 0.333), while their corresponding CCT values place them in the cool white light category. This emission balance likely arises from effective tuning of blue-to-yellow intensity ratios. Furthermore, emission branching ratios, a key factor for laser material design, were determined, with the dominant $^4F_{9/2} \rightarrow {}^6H_{13/2}$ transition contributing significantly to overall radiative decay. The luminescent behavior and tunability of these Dy(III) complexes highlight their potential as efficient single component emitters for white light applications, like white organic LEDs. In addition, their semiconducting nature suggests broader applicability in multifunctional molecular devices, including lighting systems design.

Author contributions

Vandana Aggarwal = data curation, writing – original draft; Devender Singh = writing – review & editing and supervision; Sonia Redhu = visualization; Shri Bhagwan = investigation; Sumit Kumar = validation; Rajender Singh Malik = resources; Parvin Kumar = formal analysis; Jayant Sindhu = conceptualization; Varun Kumar = software.

Conflicts of interest

The authors declare that they have no conflicts of interest.

Data availability

The authors affirm that the information/data of this research article is available inside the article.

Supplementary information (SI) is available. See DOI: https://doi.org/10.1039/d5ra05762k.

Acknowledgements

Vandana Aggarwal is thankful to UGC-New Delhi for providing JRF [221610012377].

References

1 K. Nehra, A. Dalal, A. Hooda, S. Bhagwan, R. K. Saini, B. Mari, S. Kumar and D. Singh, Lanthanides β-diketonate complexes as energy-efficient emissive materials: A review, *J. Mol. Struct.*, 2022, **1249**, 131531, DOI: 10.1016/j.molstruc.2021.131531.

2 P. P. da Rosa, Y. Kitagawa and Y. Hasegawa, Luminescent lanthanide complex with seven-coordination geometry, *Coord. Chem. Rev.*, 2020, **406**, 213153, DOI: 10.1016/j.ccr.2019.213153.

3 V. Aggarwal, D. Singh, K. Nehra, S. Dalal, S. Redhu, P. Kumar, S. Kumar and R. S. Malik, White light emission from a ternary dysprosium complex: Energy transfer and ligand-driven modulation, *Mater. Sci. Semicond. Process.*, 2025, **192**, 109427, DOI: 10.1016/j.mssp.2025.109427.

4 D. Singh, V. Tanwar, S. Bhagwan and I. Singh, Recent advancements in luminescent materials and their potential applications, *Adv. Magn. Opt. Mater.*, 2016, 317–352, DOI: 10.1002/9781119241966.ch10.

5 E. Erol, N. Vahedigharehchopogh, O. Kıbrıslı, M. Ç. Ersundu and A. E. Ersundu, Recent progress in lanthanide-doped luminescent glasses for solid-state lighting applications—A review, *J. Phys.: Condens. Matter*, 2021, **33**, 483001, DOI: 10.1088/1361-648X/ac22d9.

6 V. Aggarwal, D. Singh, A. Hooda, S. Malik, S. Dalal, S. Redhu, S. Kumar, R. S. Malik and P. Kumar, Comprehensive investigation of ternary dysprosium complexes for white light emission: Synthesis, spectroscopic and colorimetric analyses, *J. Lumin.*, 2024, **270**, 120555, DOI: 10.1016/j.jlumin.2024.120555.

7 N. Yin, Y. Yu, X. Wang, Y. Shu and J. Wang, Dual lanthanide complexes-loaded ratiometric nanothermometer for elucidating intracellular variations of temperature and calcium transport, *Chem. Eng. J.*, 2024, **490**, 151645, DOI: 10.1016/j.cej.2024.151645.

8 V. Aggarwal, D. Singh, A. Hooda, K. Nehra, K. Jakhar, S. Kumar, R. S. Malik and P. Kumar, Synthesis and photoluminescent analyses of ternary terbium(III) Tris-β-diketonate complexes: A systematic exploration, *J. Mater. Sci.:Mater. Electron.*, 2024, **35**(8), DOI: 10.1007/s10854-024-12314-z.

9 D. Parker, J. D. Fradgley and K. L. Wong, The design of responsive luminescent lanthanide probes and sensors, *Chem. Soc. Rev.*, 2021, **50**, 8193–8213, DOI: 10.1016/j.ccr.2010.04.002.

10 R. Boddula and S. Vaidyanathan, White light emissive bipolar ligand and their EuIII complex for white/red light emitting diodes, *J. Photochem. Photobiol., A*, 2017, **347**, 26–40, DOI: 10.1016/j.jphotochem.2017.07.008.

11 B. Rajamouli, P. Sood, S. Giri, V. Krishnan and V. Sivakumar, A Dual-Characteristic Bidentate Ligand for a Ternary Mononuclear Europium (III) Molecular Complex–Synthesis, Photophysical, Electrochemical, and Theoretical Study, *Eur. J. Inorg. Chem.*, 2016, **2016**, 3900–3911, DOI: 10.1002/ejic.201600508.

12 R. Boddula, J. Tagare, K. Singh and S. Vaidyanathan, White light-emissive europium complexes and their versatile applications, *Mater. Chem. Front.*, 2021, **5**, 3159–3175, DOI: 10.1039/D1QM00083G.

13 S. Maredi, S. Mund, S. R. Nayak, S. Devineni, C. Subrahmanyam and S. Vaidyanathan, White Light Emissive Eu(III) Complexes through Ligand Engineering and their Applications in Cool Near Ultraviolet White Light Emitting Diodes and Thermometer, *ChemPhysChem*, 2024, **25**, e202400320, DOI: 10.1002/cphc.202400320.

14 V. Aggarwal, D. Singh, P. Kumar, S. Dalal, S. Kumar, R. S. Malik, P. Kumar, J. Sindhu and H. Kumar, DFT Studies and Experimental Characterization of Eu^{3+} Complexes in Different Coordinating Environment: A

Comprehensive Approach to Luminescence and Applications in Display Technologies, *J. Mol. Struct.*, 2025, 142781, DOI: 10.1016/j.molstruc.2025.142781.

15 D. Singh, W. R. Buratto, J. F. Torres and L. J. Murray, Activation of dinitrogen by polynuclear metal complexes, *Chem. Rev.*, 2020, **120**, 5517–5581, DOI: 10.1021/acs.chemrev.0c00042.

16 K. M. de Souza, L. P. de Carvalho, J. A. da Silva and R. L. Longo, On the structures of dinuclear symmetric lanthanide complexes and the selectivity towards heterodinuclear complexes based on molecular modeling, *Inorg. Chim. Acta*, 2019, **494**, 65–73, DOI: 10.1016/j.ica.2019.05.009.

17 V. Aggarwal, D. Singh, S. Bhagwan, R. K. Saini, K. Jakhar, S. Kumar, P. Kumar and J. Sindhu, Tuning emissive color of trivalent terbium ion through environmental factors: optoelectronic insights from theoretical, spectral and computational studies, *RSC Adv.*, 2024, **14**, 39569–39587, DOI: 10.1039/d4ra05334f.

18 D. Singh, K. Singh, S. Bhagwan, R. K. Saini, R. Srivastava and I. Singh, Preparation and photoluminescence enhancement in terbium (III) ternary complexes with β-diketone and monodentate auxiliary ligands, *Cogent Chem.*, 2016, **2**, 1134993, DOI: 10.1080/23312009.2015.1134993.

19 L. L. Cai, S. M. Zhang, Y. Li, K. Wang, X. M. Li, G. Muller, F. P. Liang, Y. T. Hu and G. X. Wang, Lanthanide nitrato complexes bridged by the bis-tridentate ligand 2, 3, 5, 6-tetra (2-pyridyl) pyrazine: Syntheses, crystal structures, Hirshfeld surface analyses, luminescence properties, DFT calculations, and magnetic behavior, *J. Lumin.*, 2021, **232**, 117835, DOI: 10.1016/j.jlumin.2020.117835.

20 V. Aggarwal, D. Singh, A. Hooda, K. Jakhar, S. Kumar, R. S. Malik and P. Kumar, Optimizing europium (III) ion luminescence *via* β-diketone and auxiliary ligands: analysis of optoelectronic features and Judd-Ofelt parameters, *Chem. Phys. Lett.*, 2025, 142244, DOI: 10.1016/j.cplett.2025.142244.

21 Q. Liu, D. M. Wang, Y. Y. Li, M. Yan, Q. Wei and B. Du, Synthesis and luminescent properties of $Eu(TTA)_3 \cdot 3H_2O$ nanocrystallines, *Luminescence*, 2010, **25**, 307–310, DOI: 10.1002/bio.1150.

22 A. Ali, Z. Ahmed, K. Iftikhar and R. Uddin, Photophysical studies of low-symmetry Sm (iii) and Tb (iii) complexes reveal remarkable quantum yields, *New J. Chem.*, 2025, DOI: 10.1039/D5NJ01687H.

23 A. Dalal, K. Nehra, A. Hooda, D. Singh, J. Dhankhar and S. Kumar, Fluorinated β-diketone-based Sm(III) complexes: spectroscopic and optoelectronic characteristics, *Luminescence*, 2022, **37**, 1328–1334, DOI: 10.1002/bio.4300.

24 D. Singh, S. Bhagwan, R. K. Saini, V. Nishal and I. Singh, Development in organic light-emitting materials and their potential applications, *Adv. Magn. Opt. Mater.*, 2016, **32**, 473–519, DOI: 10.1002/9781119241966.ch14.

25 V. Aggarwal, D. Singh, S. Redhu, S. Malik, S. Dalal, S. Kumar, R. S. Malik, P. Kumar and J. Sindhu, Design and photophysical characterization of dinuclear lanthanide complexes incorporating spacer ligands along with their mononuclear analogues: A comparative study, *Opt. Mater.*, 2024, **155**, 115833, DOI: 10.1016/j.optmat.2024.115833.

26 A. Hooda, D. Singh, A. Dalal, K. Nehra, S. Kumar, R. S. Malik, H. Sehrawat and P. Kumar, N-donor auxiliary ligand-based terbium (III) β-diketonates: Preparation and photophysical studies, *J. Lumin.*, 2023, **258**, 119828, DOI: 10.1016/j.jlumin.2023.119828.

27 N. Ghosh, A. Bandyopadhyay, S. Roy, G. Saha and J. A. Mondal, Unified view of the hydrogen-bond structure of water in the hydration shell of metal ions (Li^+, Mg^{2+}, La^{3+}, Dy^{3+}) as observed in the entire 100–3800 cm^{-1} regions, *J. Mol. Liq.*, 2023, **389**, 122927, DOI: 10.1016/j.molliq.2023.122927.

28 V. Aggarwal, D. Singh, S. Bhagwan, R. K. Saini, K. Jakhar, R. S. Malik, P. Kumar and J. Sindhu, Exploring the influence of emissive centers in mono and dinuclear europium(III) complexes for advance lighting applications: Synthesis, characterization and computational modeling, *J. Mol. Struct.*, 2025, **1324**, 140841, DOI: 10.1016/j.molstruc.2024.140841.

29 K. Nehra, A. Dalal, A. Hooda, K. Jakhar, D. Singh and S. Kumar, Preparation, optoelectronic and spectroscopic analysis of fluorinated heteroleptic samarium complexes for display applications, *Inorg. Chim. Acta*, 2022, **537**, 120958, DOI: 10.1016/j.ica.2022.120958.

30 D. Parker, E. A. Suturina, I. Kuprov and N. F. Chilton, How the ligand field in lanthanide coordination complexes determines magnetic susceptibility anisotropy, paramagnetic NMR shift, and relaxation behavior, *Acc. Chem. Res.*, 2020, **53**, 1520–1534, DOI: 10.1021/acs.accounts.0c00275.

31 A. Hooda, D. Singh, K. Nehra, A. Dalal, S. Kumar, R. S. Malik, V. Siwach and P. Kumar, Photoluminescent Sm(III) diketonates with 1,10-phenanthroline derivatives: electrochemical and optoelectronic study, *J. Mater. Sci.: Mater. Electron.*, 2023, **34**, 1504, DOI: 10.1007/s10854-023-10899-5.

32 W. A. Dar and K. Iftikhar, Phase controlled colour tuning of samarium and europium complexes and excellent photostability of their PVA encapsulated materials, Structural elucidation, photophysical parameters and the energy transfer mechanism in the Eu^{3+} complex by Sparkle/PM3 calculations, *Dalton Trans.*, 2016, **45**, 8956–8971, DOI: 10.1039/C6DT00549G.

33 Z. Guo, Design of Multinuclear Transition Metal and Lanthanide Complexes: Magnetic and Luminescent Properties, Doctoral dissertation, University of Birmingham, 2021, http://etheses.bham.ac.uk/id/eprint/12105.

34 B. L. An, M. L. Gong, M. X. Li and J. M. Zhang, Synthesis, structure and luminescence properties of samarium(III) and dysprosium(III) complexes with a new tridentate organic ligand, *J. Mol. Struct.*, 2004, **687**, 1–6, DOI: 10.1016/S0022-2860(03)00410-1.

35 P. R. Jubu, O. S. Obaseki, F. K. Yam, S. M. Stephen, A. A. Avaa, A. A. McAsule, Y. Yusof and D. A. Otor, Influence of the secondary absorption and the vertical axis scale of the

Tauc's plot on optical bandgap energy, *J. Opt.*, 2023, **52**, 1426–1435, DOI: 10.1007/s12596-022-00961-6.

36 P. Kumar, V. Gulia and A. G. Vedeshwar, Residual stress dependant anisotropic band gap of various (hkl) oriented BaI_2 films, *Jpn. J. Appl. Phys.*, 2013, **114**, DOI: 10.1063/1.4832437.

37 P. Makuła, M. Pacia and W. Macyk, How to correctly determine the band gap energy of modified semiconductor photocatalysts based on UV-Vis spectra, *J. Phys. Chem. Lett.*, 2018, **9**, 6814–6817, DOI: 10.1021/acs.jpclett.8b02892.

38 S. Redhu, D. Singh, A. Hooda, S. Malik, V. Aggarwal, S. Dalal, S. Kumar, R. S. Malik and P. Kumar, Synthesis, characterization and luminescent properties of N-donor based samarium-tris-β-diketonate: Tuning optoelectronic characteristics for displays applications, *J. Mol. Struct.*, 2024, **1308**, 138056, DOI: 10.1016/j.molstruc.2024.138056.

39 M. R. Majewski, R. I. Woodward and S. D. Jackson, Dysprosium mid-infrared lasers: current status and future prospects, *Laser Photonics Rev.*, 2020, **14**, 1900195, DOI: 10.1002/lpor.201900195.

40 N. Kofod, R. Arppe-Tabbara and T. J. Sørensen, Electronic energy levels of dysprosium (III) ions in solution. Assigning the emitting state and the intraconfigurational 4f–4f transitions in the Vis–NIR region and photophysical characterization of Dy (III) in water, methanol, and dimethyl sulfoxide, *J. Phys. Chem. A*, 2019, **123**, 2734–2744, DOI: 10.1021/acs.jpca.8b12034.

41 W. M. Wang, W. Z. Qiao, H. X. Zhang, S. Y. Wang, Y. Y. Nie, H. M. Chen, Z. Liu, H. L. Gao, J. Z. Cui and B. Zhao, Structures and magnetic properties of several phenoxo-O bridged dinuclear lanthanide complexes: Dy derivatives displaying substituent dependent magnetic relaxation behavior, *Dalton Trans.*, 2016, **45**, 8182–8191, DOI: 10.1039/C6DT00220J.

42 A. Dalal, K. Nehra, A. Hooda, D. Singh, P. Kumar, S. Kumar, R. S. Malik and B. Rathi, Luminous lanthanide diketonates: Review on synthesis and optoelectronic characterizations, *Inorg. Chim. Acta*, 2023, **550**, 121406, DOI: 10.1016/j.ica.2023.121406.

43 W. M. Wang, S. Y. Wang, H. X. Zhang, H. Y. Shen, J. Y. Zou, H. L. Gao, J. Z. Cui and B. Zhao, Modulating single-molecule magnet behaviour of phenoxo-O bridged lanthanide (III) dinuclear complexes by using different β-diketonate coligands, *Inorg. Chem. Front.*, 2016, **3**, 133–141, DOI: 10.1039/C5QI00192G.

44 A. Kuznetsova, V. Matveevskaya, D. Pavlov, A. Yakunenkov and A. Potapov, Coordination polymers based on highly emissive ligands: Synthesis and functional properties, *Material*, 2020, **13**, 2699, DOI: 10.3390/ma13122699.

45 W. M. Wang, X. M. Kang, H. Y. Shen, Z. L. Wu, H. L. Gao and J. Z. Cui, Modulating single-molecule magnet behavior towards multiple magnetic relaxation processes through structural variation in Dy_4 clusters, *Inorg. Chem. Front.*, 2018, **5**, 1876–1885, DOI: 10.1039/C8QI00214B.

46 W. Chu, Q. Sun, X. Yao, P. Yan, G. An and G. Li, Luminescent single molecule magnets of a series of β-diketone dysprosium complexes, *RSC Adv.*, 2015, **5**, 94802–94808, DOI: 10.1039/c5ra17358b.

47 J. Zhong, J. Tang, C. Ye and L. Dong, The immunology of COVID-19: is immune modulation an option for treatment?, *Lancet Rheumatol.*, 2020, **2**, e428–e436.

48 J. F. Chen, Y. L. Ge, D. H. Wu, H. T. Cui, Z. L. Mu, H. P. Xiao, X. Li and J. Y. Ge, Two-dimensional dysprosium(III) coordination polymer: Structure, single-molecule magnetic behavior, proton conduction, and luminescence, *Front. Chem.*, 2022, **10**, 974914, DOI: 10.3389/fchem.2022.974914.

49 V. Aggarwal, D. Singh, S. Malik, S. Bhagwan, S. Kumar, R. S. Malik, P. Kumar and J. Sindhu, Highly emissive dinuclear europium(iii) complex with heteroaryl β-diketone and fluxidentate pyrazine: dual role as UV converters and semiconductors, *RSC Adv.*, 2025, **15**, 44102–44115, DOI: 10.1039/D5RA06968H.

50 S. Dalal, D. Singh, A. Dalal, A. Hooda, S. Kumar, R. S. Malik, P. Kumar and J. Sindhu, Green emissive Tb(III) complexes based on photosensitizing antenna: Synthesis and optoelectronic analysis, *Mater. Sci. Semicond. Process.*, 2024, **177**, 108370, DOI: 10.1016/j.mssp.2024.108370.

51 W. M. Wang, H. X. Zhang, S. Y. Wang, H. Y. Shen, H. L. Gao, J. Z. Cui and B. Zhao, Ligand field affected Single-Molecule Magnet behavior of lanthanide (III) dinuclear complexes with an 8-hydroxyquinoline Schiff base derivative as bridging ligand, *Inorg. Chem.*, 2015, **54**, 10610–10622, DOI: 10.1021/acs.inorgchem.5b01404.

52 V. Aggarwal, D. Singh, A. Hooda, K. Nehra, S. Redhu, S. Kumar, R. S. Malik and P. Kumar, Design and spectroscopic study of samarium complexes with tunable photoluminescent properties, *J. Mol. Struct.*, 2024, **1311**, 138315, DOI: 10.1016/j.molstruc.2024.138315.

53 A. Dalal, K. Nehra, A. Hooda, D. Singh, S. Kumar and R. S. Malik, Red emissive ternary europium complexes: synthesis, optical, and luminescence characteristics, *Luminescence*, 2022, **37**, 1309–1320, DOI: 10.1002/bio.4297.

54 W. A. Dar, Z. Ahmed and K. Iftikhar, Cool white light emission from the yellow and blue emission bands of the Dy(III) complex under UV-excitation, *J. Photochem. Photobiol., A*, 2018, **356**, 502–511, DOI: 10.1016/j.jphotochem.2017.12.017.

55 Z. Ahmed and K. Iftikhar, Efficient layers of emitting ternary lanthanide complexes for fabricating red, green, and yellow OLEDs, *Inorg. Chem.*, 2015, **54**, 11209–11225, DOI: 10.1021/acs.inorgchem.5b01630.

56 P. A. Tanner, W. Thor, Y. Zhang and K. L. Wong, Energy transfer mechanism and quantitative modeling of rate from an antenna to a lanthanide ion, *J. Phys. Chem. A*, 2022, **126**, 7418–7431, DOI: 10.1021/acs.jpca.2c03965.

57 Y. He, G. Fu, L. Liu, H. Li, B. Li, J. Guan, X. Lü, W. K. Wong and R. A. Jones, First example of PMMA-supported and highly luminous color-purity red-light metallopolymer based on a tris-β-diketonate Zn^{2+}-Eu^{3+}-complex, *Inorg. Chem. Commun.*, 2016, **69**, 62–65, DOI: 10.1016/j.inoche.2016.04.027.

58 K. Remmers, R. G. Satink, G. von Helden, H. Piest, G. Meijer and W. L. Meerts, Gas-phase infrared spectroscopy on the

lowest triplet state of the pyrazine–argon complex, *Chem. Phys. Lett.*, 2000, **317**, 197–202, DOI: 10.1016/S0009-2614(99)01387-1.

59 L. Wu, X. D. Huang, W. Li, X. Cao, W. H. Fang, L. M. Zheng, M. Dolg and X. Chen, Lanthanide-Dependent Photochemical and Photophysical Properties of Lanthanide–Anthracene Complexes: Experimental and Theoretical Approaches, *JACS Au*, 2024, **4**, 3606–3618, DOI: 10.1021/jacsau.4c00540.

60 S. Redhu, D. Singh, S. Dalal, S. Malik, V. Aggarwal, A. Hooda, S. Kumar, R. S. Malik and P. Kumar, Synthesis and comprehensive analysis of luminescent dysprosium(III) complexes: Photoluminescence, thermal behavior and electrochemical properties, *Polyhedron*, 2024, **261**, 117146, DOI: 10.1016/j.poly.2024.117146.

61 J. Li, X. Zhang, B. Yue, A. Wang, L. Kong, J. Zhou, H. Chu and Y. Zhao, Preparation, Crystal structure and Luminescence Properties of Lanthanide Complexes with 2,4,6-tri(pyridin-2-yl)-1,3,5-triazine and Organic Carboxylic Acid, *Crystal*, 2017, **7**, 139, DOI: 10.3390/cryst7050139.

62 P. Kumar, D. Singh, S. Kadyan, H. Kumar and R. Kumar, Cool green-emissive $Y_2Si_2O_7$:Tb^{3+} nanophosphor: auto-combustion synthesis and structural and photoluminescence characteristics with good thermal stability for lighting applications, *RSC Adv.*, 2024, **14**, 16560–16573, DOI: 10.1039/D4RA02571G.

63 R. Malik, K. Ray and S. Mazumdar, A low-cost, wide-range, CCT-tunable, variable-illuminance LED lighting system, *Leukos*, 2020, DOI: 10.1080/15502724.2018.1541747.

64 G. Ozenen, *Architectural Interior Lighting*. Springer, 2023, DOI: 10.1007/978-3-031-49695-0.

65 V. Sivakumar and B. Rajamouli, *Molecular Designing of Luminescent Europium-Metal Complexes for OLEDs: an Overview*, Phosphors, 2018, 325–404.

66 E. Berti, A. Caneschi, C. Daiguebonne, P. Dapporto, M. Formica, V. Fusi, L. Giorgi, A. Guerri, M. Micheloni, P. Paoli and R. Pontellini, Ni (II), Cu (II), and Zn (II) Dinuclear Metal Complexes with an Aza−Phenolic Ligand: Crystal Structures, Magnetic Properties, and Solution Studies, *Inorg. Chem.*, 2003, **42**, 348–357, DOI: 10.1021/ic0204070.

67 X. Feng, J. L. Chen, L. Y. Wang, S. Y. Xie, S. Yang, S. Z. Huo and S. W. Ng, A series of homonuclear lanthanide complexes incorporating isonicotinic based carboxylate tectonic and oxalate coligand: structures, luminescent and magnetic properties, *CrystEngComm*, 2014, **16**, 1334–1343, DOI: 10.1039/C3CE41674G.